The accuracy of a new approach to order determination for the Modified Prony method in swath mapping application

Piotr GRALL

Gdańsk University of Technology
Faculty of Electronics, Telecommunications and Informatics
Department of Marine Electronic Systems
Narutowicza 11/12,80-233 Gdańsk, Poland
grallu@poczta.onet.pl

This article presents the performance of a new approach to determine the model order for the modified Prony method applied to swath acoustic mapping. Key requirements for any mapping application are depth determination accuracy and angular resolution. Depth determination accuracy is strictly related to angular accuracy and geometrical relations between receiver and sources of the backscattered signal. Angular resolution determines detection capabilities of targets laying on the seafloor. Performance of the proposed method, in terms of these two parameters, is tested against a simulated signal in a number of generic configurations, and compared to the results of other methods applied to the same signal.

Keywords: swath bathymetry, principal components, resolution, DOA.

1. Introduction

The Modified Prony (MP) method for Direction-of-Arrival (DOA) is reported to perform with similar accuracy to the Maximum Likelihood method for static DOAs, provided a large number of receivers are available [10]. Backscattered signals present in underwater mapping applications are expected to be highly non-stationary, though, meaning constant change of DOA at a variable rate [9]. For this reason, vertical angular accuracy in the x-z plane (Fig.1) of the MP method is expected to deviate from the results obtained for stationary signals. Additionally, propagation effects, characteristic for swath bathymetry, such as baseline decorrelation and shifting (sliding) footprint lower element-to-element signal coherence which, in turn lowers the equivalent Signal-to-Noise ratio (SNR), and thus degrades accuracy [3, 7]. Finally, angular accuracy, influences achievable depth determination accuracy, which specifies to what extent a bathymetric system is efficient in hydrographic applications [12]. Knowing the accuracy of DOA and other devices composing the hydrographic system, its performance might assessed for compliance with International Hydrographic Organization Standards [1].

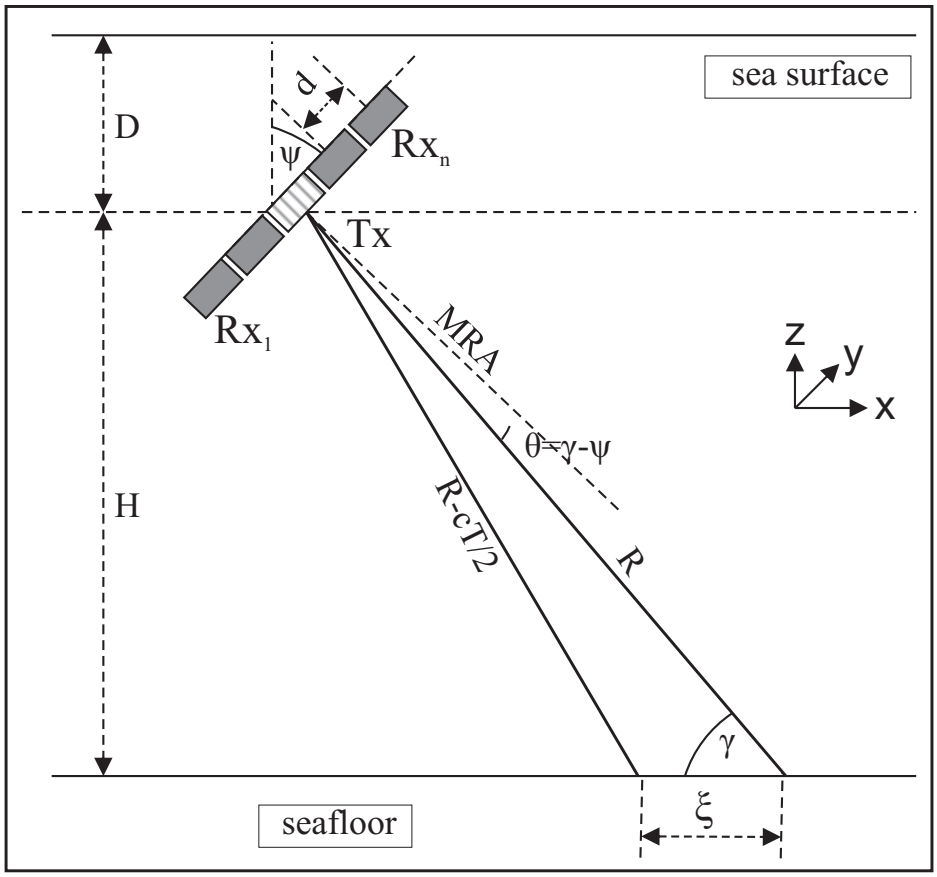

Fig. 1. Basic geometrical relations of the simulated seafloor.

Another important requirement for a bathymetric system is its detection capability of objects laying on the seafloor. The MP method is capable of simultaneously determining multiple DOAs [4–6]. It is known, however, that resolution of modern high-resolution methods is SNR-dependent [10]. Resolution is defined as "the degree of ability of a system to indicate separately the echoes of two targets in range and bearing" [11]. For a swath mapping application discrimination against angular separation is of the most importance, due to overlay effects. Angular resolution can be defined as the ability of a method to discern two closely spaced targets at the same range, laying in the same vertical plane x-z as the main response axis (MRA) - Fig.1. This parameter is equivalent to receive across-track beamwidth of multi-beam echosounders. Since no beamforming is performed in swath bathymetry, angular resolution is not only dependent on the physical array size, but also on the available SNR and applied signal processing method.

In this article, the two above-mentioned parameters, angular accuracy and angular resolution, are tested in simulated generic target-receiver configurations to assess the performance of the MP method, and a new model order determination method proposed in a related article [2]. The performance of the MP method is also compared to the performance of Least Squares (LS) and Total Least Squares (TLS) methods applied for the same simulated signal.

2. Prony problem formulation

In the Prony method the following assumptions are made (Fig.1) [4]:

1. A linear N-element equispaced array is used to measure backscatter arrivals propagating in the same plane as the array.
2. At each instant in time exactly M independent, coplanar plane waves are incident on the receiving array (M distinct backscatter sources).
3. The acoustic backscatter is narrowband.
4. The receiving array output signals are in steady state across the entire array.

The signal received at a single hydrophone, at a given instant, can be expressed as:

$$s(n) = \sum_{i=1}^{M} a_i \, e^{(\alpha_i + j\, u_i)\, d\,(n-1)} + w(n) \tag{1}$$

$$a_i = A_i \, e^{j\Theta_i},\; u_i = k \sin\theta_i \;, n = 1, 2, 3, \cdots, N$$

where u_m is the acoustic wavenumber, $k = 2\pi/\lambda$, λ is the wavelength at the central frequency, α_i, θ_i and a_i are time dependent exponential damping factor, DOA, and complex amplitude respectively, associated with the *i*-th backscattering source, and $w(n)$ is additive noise at each array element. Distance between receive elements should satisfy inequality: $d \leq \lambda/2$.

We might find DOAs of the backscattered signals by solving equivalent problem of digital linear prediction-error filter design i.e. computing complex roots of the polynomial ([8, 10]):

$$H(z) = 1 + \sum_{l=1}^{L} g_l \, z^{-l} = 0 \tag{2}$$

where L is called filter order and $z = e^{\sigma + j\omega}$. If L satisfies the inequality:

$$M \leqslant L \leqslant (N - M/2) \tag{3}$$

complex coefficients g_l may be obtained by solving a set of linear complex forward–backward equations [10]:

$$\begin{bmatrix} s(L) & s(L-1) & \cdots & s(1) \\ s(L+1) & s(L) & \cdots & s(2) \\ \vdots & \vdots & & \vdots \\ s(N-1) & s(N-2) & \cdots & s(N-L) \\ \hline s^*(2) & s^*(3) & \cdots & s^*(L+1) \\ s^*(3) & s^*(4) & \cdots & s^*(L+2) \\ \vdots & \vdots & & \vdots \\ s^*(N-L+1) & s^*(N-L+2) & \cdots & s^*(N) \end{bmatrix} \begin{bmatrix} g_1 \\ g_2 \\ \vdots \\ g_L \end{bmatrix} = - \left[\begin{array}{c} s(L+1) \\ s(L+2) \\ \vdots \\ s(N) \\ \hline s^*(1) \\ s^*(2) \\ \vdots \\ s^*(N-L) \end{array}\right] \tag{4a}$$

or shortly:

$$Ag = -h \tag{4b}$$

where * denotes a complex conjugate. Out of L roots of the eq.(2) M closest to the unit circle on the complex plane are equal to $e^{(\alpha_i + j\,u_i)\,d}$ components in eq.(1) and DOAs of interest can be determined. Additional $L - M$ roots lying further away from the unit circle are rejected. If $M = L$ no additional roots of eq.(2) exist.

For a large number of receive elements we can choose L to be any value from the interval defined by eq.(3). This situation leads to the following question:

Is there an optimal value of L, with respect to M and N, that gives the most accurate estimates of DOAs?

Some authors [4] suggest to choose initially the largest possible value of L and decrease it in each step of iteration until the number of roots z_0 of eq.(2) closest to the unit circle (within $1 \pm \delta$ interval, where δ is an a priori specified distance from the unit circle) reaches the convergence criterion. An other approach would be to first estimate the number of reflection sources M and set $M = L$. Once L is set, eq.(4a) can be solved using well-known methods such as Least-Square (LS) or Total-Least Squares (TLS) methods.[1]

The Modified Prony method, as proposed by Tufts and Kumaresan [10], suggests to choose a fixed $L \approx \frac{3}{4}N$, to obtain best DOA estimates, if the number of sources M is much smaller than N. This method requires one to first assess the number of signals, and then perform a low-rank approximation of correlation matix:

$$g = \hat{g} = \sum_{i=1}^{M} \frac{u_i^* r\, u_i}{\gamma_i} \tag{5}$$

where:

$$r = -A^* h \tag{6}$$

$$R = A^* A = U \Lambda\, U^* \tag{7}$$

Eq.(7) describes eigenvalue/eigenvector decomposition of R, γ_i are the eigenvalues of R sorted in descending order, situated on the main diagonal of Λ. The column vectors of U i.e u_i are orthonormal eigenvectors of R. The low-rank approximation requires rejecting $M - L$ smallest eigenvalues of R by explicitly setting them to "0", as would be expected for the correlation matrix of M signals not affected by noise.

The advantage of the Modified Prony method is that the sizes of the matrix and vectors in eq.(4a) are fixed: thus providing very predictable commutation time, and does not require iterations, which makes it favourable for on-line processing and multithreading programming. In the following sections the above-described methods for solving eq.(4a) will be compared in terms of angular accuracy and angular resolution.

3. Simulation methodology

The number of receiver elements N in all simulations is set to 12. For the MP method L is equal to 9 which is exactly $\frac{3}{4}$ of N [10]. Receiver elements are assumed to have the same characteristics (cosine elements) and no cross-talk between them. The projector has the

[1] Using the TLS method forces all zeros of eq.(2) to be on the unit circle on the complex plane.

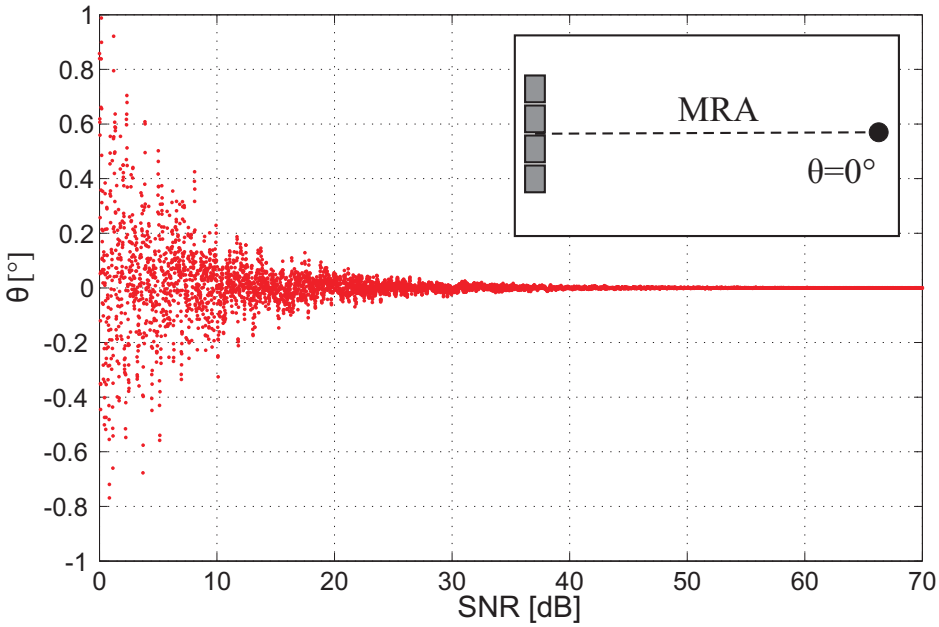

Fig. 2. Test-1 configuration and sample simulation results. DOA estimates as a function of SNR.

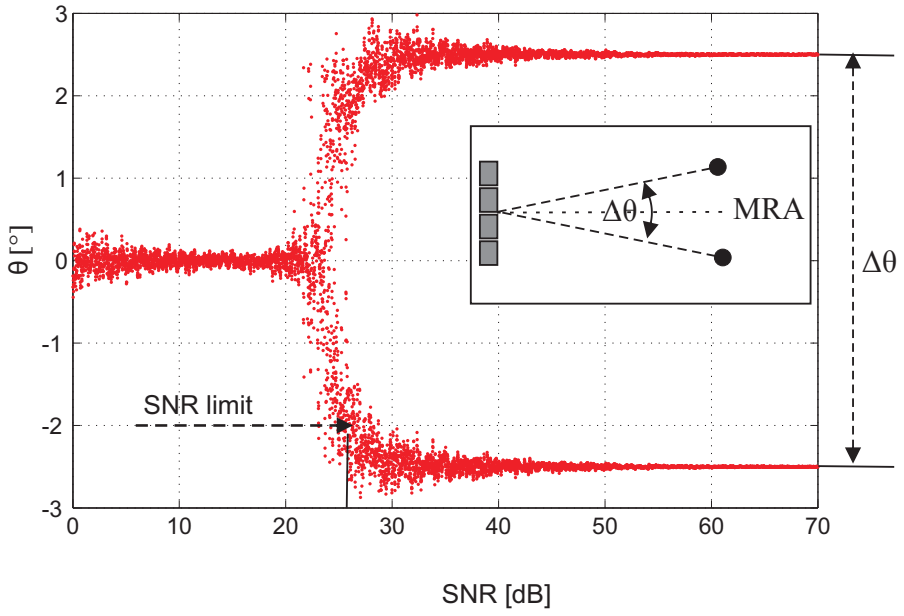

Fig. 3. Test-2 configuration and sample simulation results for angular separation $\Delta\theta = 5°$. DOAs estimates as a function of SNR. Arrow indicates assumed resolution limit.

same directional characteristic as a single receive element (no beamforming is performed on transmit nor receive, which is a general rule of swath bathymetry) and is located in the middle of the array. In a real system the projector is separated in space from receive elements in the y direction (Fig.1).

In Test-1 a single point perfectly reflecting target is simulated i.e. no propagation loss nor attenuation is included (Fig.2). The target is situated exactly on the main response axis (MRA)

in the far field of the array. At each time, each array element receives the same signal with a given complex sine wave amplitude and random phase. Each element input is perturbed then by complex additive white Gaussian noise with the Rayleigh parameter $b = \sigma$.

$$s(n) = A\, e^{j\phi} + w(n) \tag{8}$$

where A and σ are chosen to obtain the desired SNR:

$$SNR = 20 \log_{10} \frac{A}{2\sigma} \tag{9}$$

Multiple samples are taken for fixed SNR to assess angular accuracy of different methods. Complex sine amplitude A is subsequently varied with σ remaining fixed, to test angular accuracy for SNR ranging from 0 to 70 dB. For the LS method the value of L changes between 1 and 4, for the the TLS method $L = 1$.[2] This simulation configuration serves as a benchmark for accuracy achievable by each method in relation to SNR. It neglects propagation loss, attenuation, reflectivity directivity patterns of transmit and receive elements and phenomena related to sonar signal propagation such as shifting footprint effect and baseline decorrelation, and changes of DOA in time. Results represent the maximum achievable accuracy against Gaussian noise for a given method in relation to SNR, and for the number of snapshots K and number of receive elements N specified.

In Test-2 angular resolution of different methods is assessed. Simulation configuration is similar to Test-1, but this time there are two perfectly reflecting targets separated by angle $\Delta\psi$ (Fig.3) and situated symmetrically around MRA.

$$s(n) = A\, e^{j(\phi_1 + \phi(n, \Delta\theta/2))} + A\, e^{j(\phi_2 - \phi(n, \Delta\theta/2))} + w(n) \tag{10}$$

where ϕ_1, θ_2 are random phases of target 1 and 2 respectively, and $\phi(n, \Delta\theta/2)$ is phase delay in relation to the centre of the array, calculated for the n-th receiver and separation angle $\Delta\psi$.

The value SNR when the 2 sources cannot be distinguished properly is taken as the limiting value for the given separation angle (Fig.3). For LS method the value of L changes between 2 and 4, for TLS method $L = 2$.

Test-3 represents a more realistic configuration (simulation parameters in Tab.1). The seafloor backscattering is simulated to give signal characteristic for scattering from rough surface (Rayleigh scattering). Bottom consists of random elements uniformly distributed at the depth H with scattering density $SD = 200m^{-1}$. All scatterers are assumed to by in the x-z plane. Horizontal receive element directivity is included, though, in calculating the echo level. At first, each scatterer has equal amplitude of 1 V and random initial phase ϕ_i (uniformly distributed). Amplitude of a given scatterer is than scaled by the range scaling factor calculated for footprint echo level according to active sonar equation: [3]

$$20 \log_{10} G(R) = SL - TL(R) + TS + BS(R) + B_{tx}(R) + B_{rx}(R) - 10 \log_{10}(SD \cdot \xi) + OCV \tag{11}$$

[2] For $L > 4$ accuracy degrades significantly.

[3] Echo level :$EL = SL - TL(R) + TS + BS(R) + B_{tx}(R) + B_{rx}(R)$ [6].

$$
\begin{aligned}
where: R = \frac{ct}{2} &- \textit{range, t- two-way impulse travel time}\\
G(R) &- \textit{range scaling factor } V/V\\
SL &- \textit{source level}\\
TL = 40\log_{10}(R) + 2\alpha R &- \textit{transmission loss}\\
\alpha &- \textit{absorbtion coefficient}\\
TS &- \textit{seafloor backscattering strength constant}\\
BS = 20\log_{10}(\sin\gamma(R)) + 10\log_{10}(A)&\\
\gamma = \arcsin(H/R) &- \textit{grazing angle at the botoom}\\
\theta = \gamma - \psi &- \textit{angle of incidence at the receiver relative to MRA}\\
A = \xi\,\theta_{3dB}\,R &- \textit{area of infonified bottom}\\
\theta_{3dB} &- \textit{horizontal 3dB beamwidth}\\
\xi = \sqrt{R^2 - H^2} - \sqrt{\left[R - (c\tau/2)\right]^2 - H^2} &- \textit{effective footprint length}\\
B_{tx} = B_{rx} = 10\log_{10}(\cos\theta) &- \textit{transmitter/receivers beampattern}\\
\psi &- \textit{array tilt ,}\\
SD &- \textit{scattering density}\\
OCV &- \textit{array element open circuit voltage response}
\end{aligned}
$$

Amplitude is multiplied by the scale factor $G(R)$, phase delay $\phi(n,i)$ is calculated for the distance from projector to the bottom element and back from the bottom element to each receive element and added to the initial phase ϕ_i. Each bottom element contributes to the receive element response as long as it is within the footprint ξ for a given range R:

$$s(n,R) = \sum_{i=1}^{k} \sqrt{2}\cdot G(R)\, e^{j(\phi_i + \phi(n,i))} \tag{12}$$

Subsequently, complex additive white noise with the Rayleigh parameter $b = 1\mu V$ is added to the output of each receive element. Finally time-varied gain (TVG) :

$$20\log_{10}(TVG(R)) = 40\log_{10}(R) + 2\alpha R \ \text{ dB resp. 1 m} \tag{13}$$

is applied to simulate signal voltage output consistent with the one expected in a real sonar system. The expected and sample simulated SNR as a function of x direction is displayed in Fig.4 for array altitude $H = 10$, and $SL = 200\,dB$. The received signal has the desired mean SNR value, while exhibiting variability characteristic for fully developed speckle noise.

Test-4 represents a configuration similar to Test-3, but this time another source of backscattering is added above the receive array at height equal to H. This surface simulates the multipath signal reflected first from bottom and then from the sea surface. For simplicity, this surface is of equal backscattering strength to bottom surface. Sea surface direct reflection influence is neglected because its contribution vanishes rapidly with range due to the low grazing angle ($D = 1\,m$). In Tests 3 and 4 the number of signals for the MP method is assessed using the method proposed in a related article [2]. This method dynamically determines the limiting eigenvalue for low-rank approximation using equivalent noise calculation. This number

Tab. 1. Simulation parameters

Parameter Name	Value
Depth (D)	1 m
Altitude (H)	10 m
Depression Angle (ψ)	25°
Frequency	200 kHz
Pulse Length – Rectangular (τ)	100 µs
Horizontal Beamwidth (θ_{3dB})	1.5°
Receive Elements (N)	12
Filter Order (L)	1,2,3,4,9
Number of snapshots (K)	5
Sample Rate	25 kHz
SL	200 dB resp. $1\,\mu\mathrm{Pa}$ at 1 m
NL	71 dB resp. $1\,\mu\mathrm{Pa}$ at 1 m
TS	-29 dB
OCV	-191 dB resp. $1\mathrm{V}/1\,\mu\mathrm{Pa}$ at 1 m
Noise Floor = NL+OCV	1 µVrms
Scattering Density (SD)	200 m^{-1}
Sound Speed (c)	1486 m/s
Sound Absorption (α)	0.05 dB/m

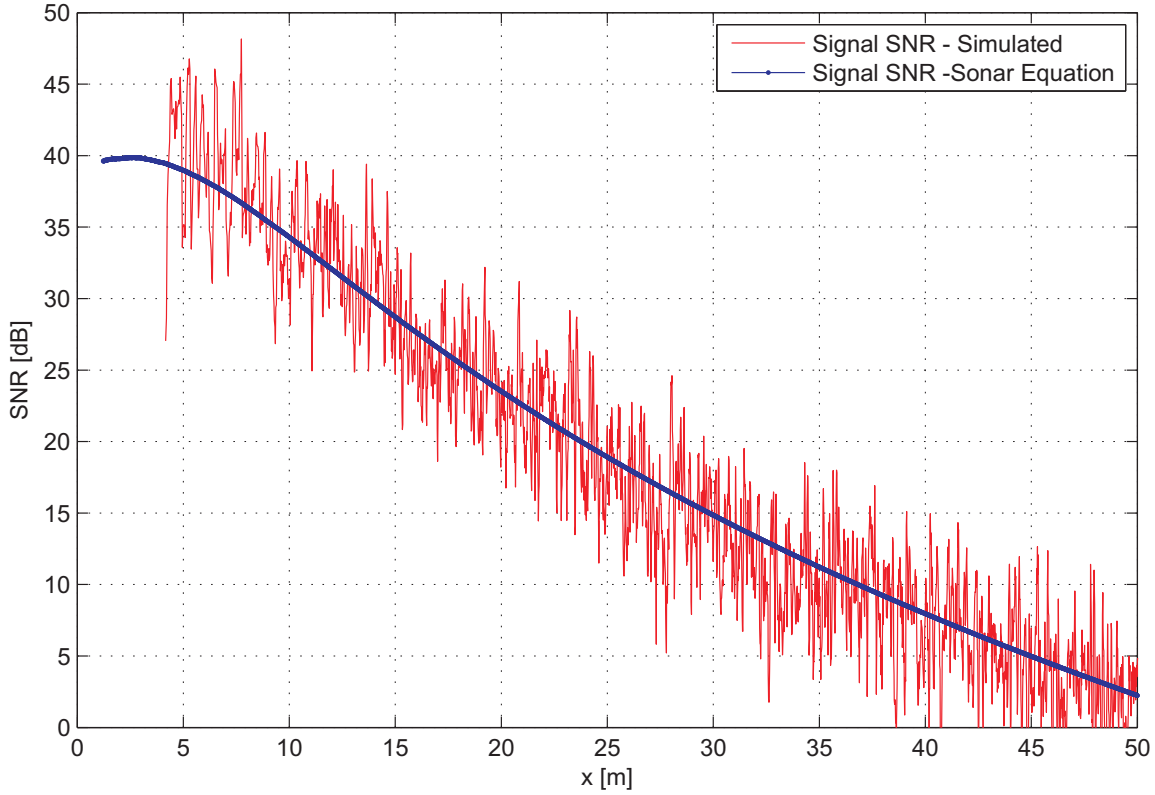

Fig. 4. Simulated and expected SNR in Test-3 for horizontal bottom configuration, $H = 10m$.

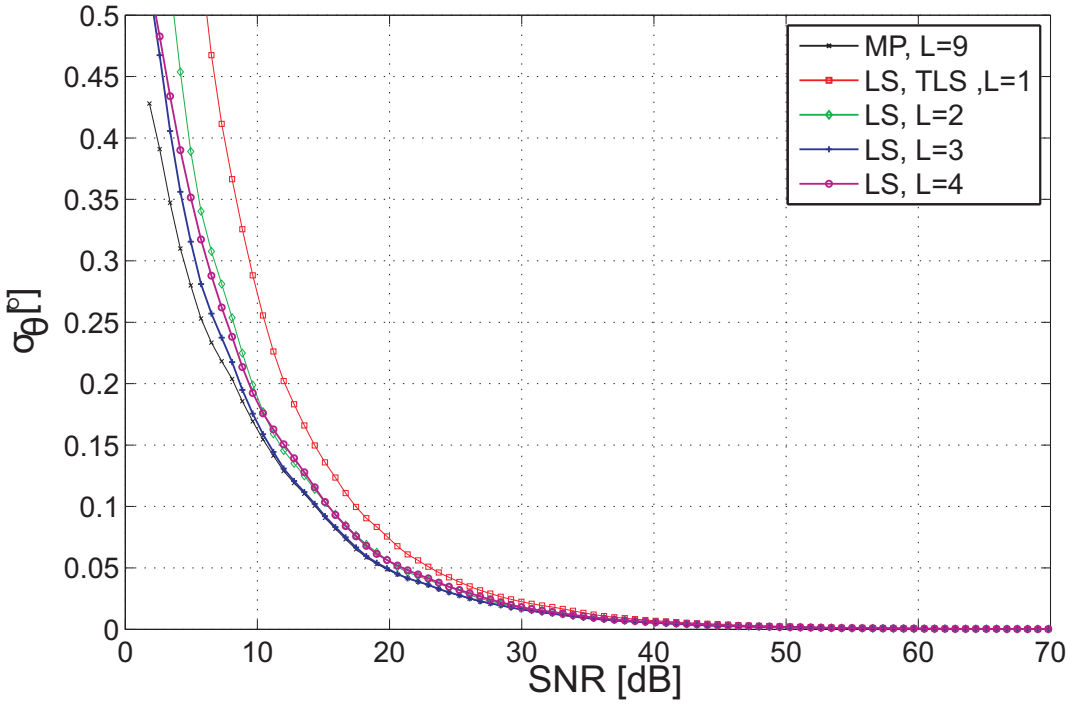

Fig. 5. Results of Test-1. Angular accuracy of different methods as a function of SNR. All results are calculated for $K = 5$.

might, of course, be determined directly from the simulation configuration $M = 1$ and $M = 2$ respectively, but the aim of the simulation, apart from accuracy assessment, is to validate the method's ability to correctly assess the number of incoming signals.

4. Simulation results

In Test-1 angular accuracy decreases with decreasing SNR (Fig.5). At first, accuracy increases with increasing L for LS method, but for $L \geq 4$ accuracy starts to decrease as additional zeros of eq.(2) are situated closer to the unit circle on the complex plane. The MP method gives better accuracy than the best of LS methods for the whole range of SNR tested, i.e exhibits lower SNR threshold effect.The TLS method gives results identical to $LS, L = 1$ and is not displayed in Fig.5 for clarity reasons. For $SNR > 12\,dB$ angular accuracy is better than $0.2°$ for all tested methods except for $L = 1$. Differences between methods are significant for $SNR < 30dB$.

In Test-2 angular resolution also decreases with decreasing SNR (Fig.6). At first, resolution increases with increasing L for LS method, but for $L > 4$ resolution starts to decrease as additional zeros of eq.(2) are situated closer to the unit circle on the complex plane. The MP method gives better resolution than the best LS method for the whole range of tested SNR. The TLS method gives results identical to $TS, L = 2$ and is not displayed in Fig.6 for clarity reasons.

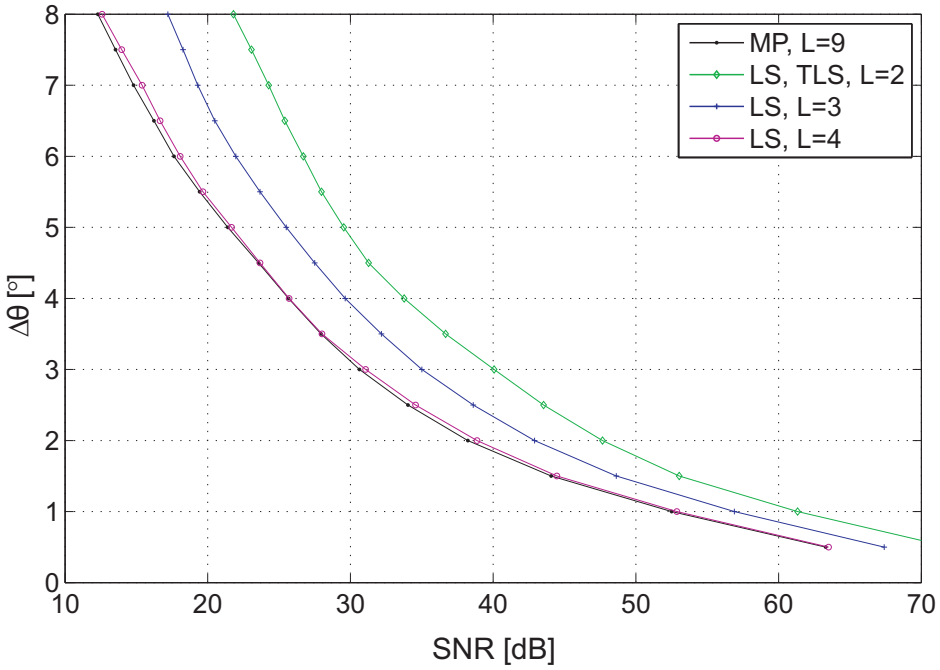

Fig. 6. Results of Test-2. Angular resolution of different methods as a function of SNR. All results are calculated for $K = 5$.

Results of Test-3 display the characteristic behaviour of swath bathymetry. Depth determination accuracy σ_H is directly related to angular accuracy σ_θ. As SNR and DOA of the incoming signal changes, the depth determination accuracy changes as well. The dependence between depth error and angular error, for flat bottom assumption, can be calculated from the formula (neglecting range inaccuracy):

$$\sigma_z = H \cot(\gamma)\, \sigma_\theta \tag{14}$$

For comparison, results inferred from Test-1 for accuracy are also plotted for the MP method. Differences between Test-1 and Test-3 are caused by the factors mentioned in Section 3. Depth determination accuracy in swath bathymetry is low in the nadir direction. With the decreasing grazing angle, accuracy improves and is the best for directions near MRA, and then again degrades along with decreasing SNR (Fig.7). Again, the MP method performs better than other methods, for low SNR values (confront Fig.4).

Results of Test-4 depict performance of the selected methods in the presence of strong multipath (Fig.8). Accuracy results are similar to Test-3, but the improvement of accuracy of the MP in relation to other methods is more significant. The best accuracy was obtained for the LS method with $L = 3$. Still, its performance was slightly worse than the MP method using low-rank approximation. The other methods tested for the same input signal (TLS and LS with various filter order) performed similarly for close ranges (higher SNR). For larger ranges, past the MRA, each of these methods perform worse than the proposed approach. In the nadir region the proposed method is not efficient enough in setting eigenvalues limits, which indicates the possible need of minor refinements.

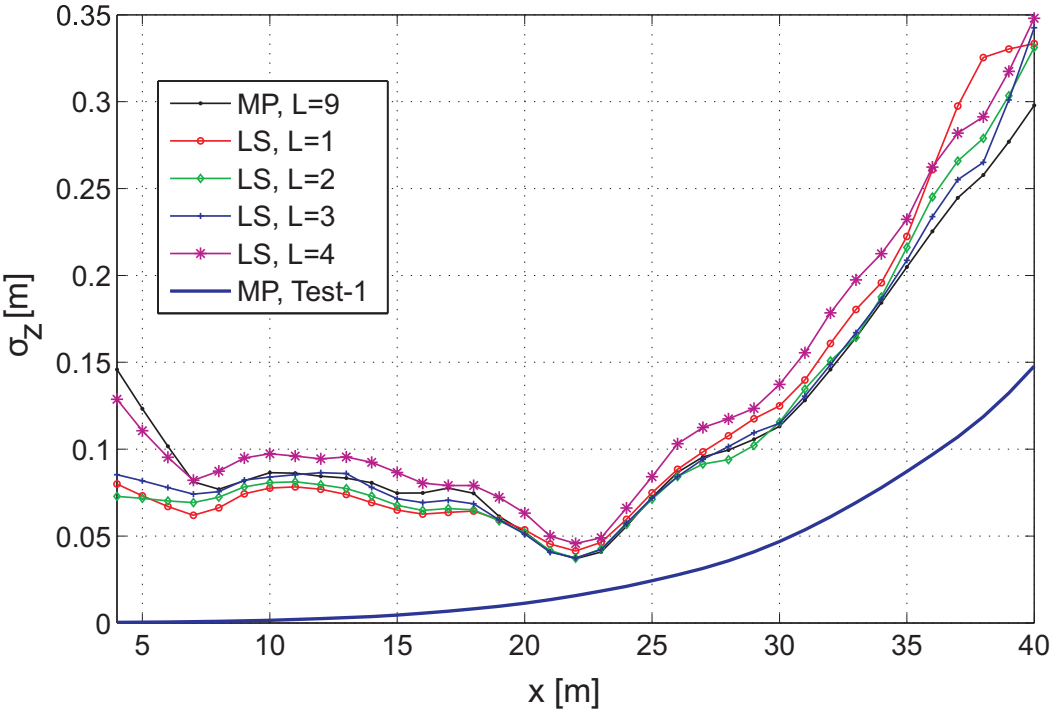

Fig. 7. Results of Test-3. Depth determination accuracy as a function of cross-track distance x. $M = 1$. All results are calculated for $K = 5$, $H = 10\,m$.

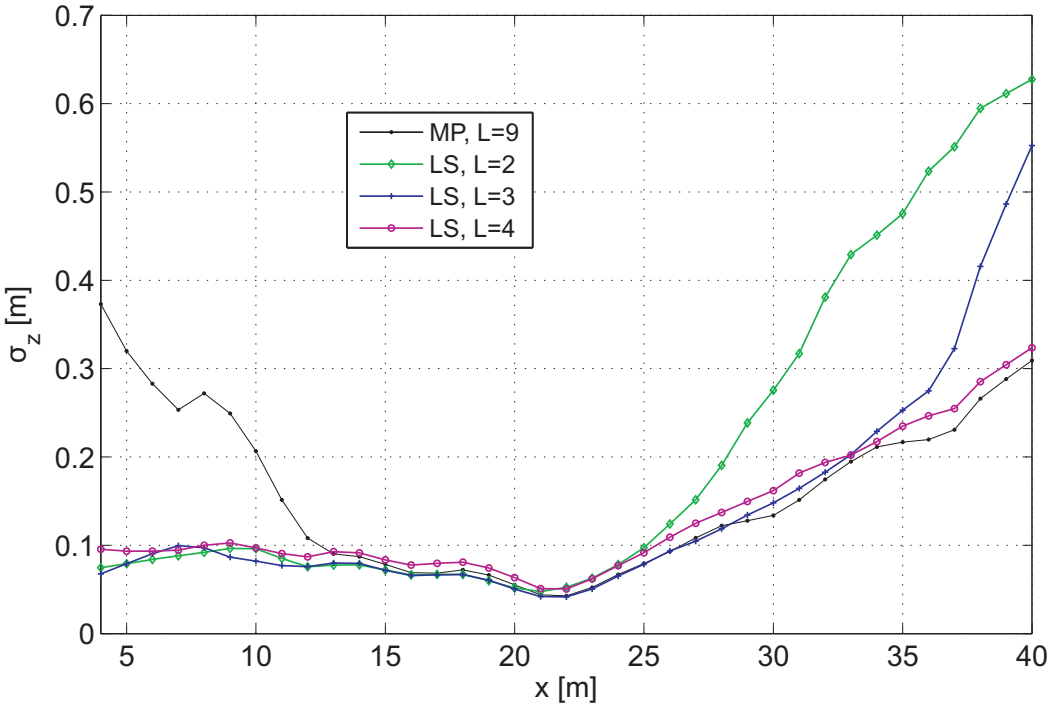

Fig. 8. Results of Test-4. Depth determination accuracy as a function of cross-track distance x. $M = 2$ All results are calculated for $K = 5$, $H = 10\,m$.

5. Conclusions

This article presented the performance of the Modified Prony method applied to the underwater DOA estimation. The results of the proposed method are superior to the other methods applied to the same signal, provided the number of incoming signals is resolved properly. The proposed method exhibits lower "threshold effect" than other methods as well. As a result, a larger final swath range of acceptable accuracy can be achieved, rendering hydrographic research more efficient. For very high SNR angular resolution is comparable to modern multi-beam echosounders (of order of 2°) but degrades significantly with SNR, lower than 40 dB. The proposed method for number of sources determination for the Modified Prony method will be further tested for its accuracy and detection capabilities as defined in the IHO standards in a more complicated acoustical environment, and for real data acquired during sea surveys.

References

[1] P. Grall, J. Marszal, Investigation into Interferometric Sonar System Accuracy, Hydroacoustics, vol. 18, pp 69-76, 2015.

[2] P. Grall, J. Marszal, Theoretical Analysis of a New Approach to Order Determination for the Modified Prony Method in Swath Mapping Application, Hydroacoustics, vol. 20, 2017.

[3] G. Jin, D. Tang, Uncertainties of Differential Phase Estimation Associated with Interferometric Sonars, IEEE Journal of Oceanic Engineering, vol. 21, no. 1, pp 53-64, 1996.

[4] P. H. Kraeutner, J. S. Bird, Principal Components Array Processing for Swath Acoustic Mapping, Proc. of the IEEE Oceans'97 Conference, pp 1246-1255, 1997.

[5] P. H. Kraeutner, J. S. Bird, Beyond Interferometry, Resolving Multiple Angles-of Arrival in Swath Bathymetric Imaging, Proc. of the IEEE Oceans'99 Conference, pp 37-46, 1999.

[6] P. H. Kraeutner, J. S. Bird, B. Charbonneau, D. Bishop, F. Hegg, Multi-Angle Swath Bathymetry Sidescan Performance Analysis, Proc. of the IEEE Oceans'02 Conference, pp 2253-2264, 2002.

[7] X. Lurton, Swath Bathymetry Using Phase Difference: Theoretical Analysis of Acoustical Measurement Precision, IEEE Journal of Oceanic Engineering, vol. 25, no. 3, pp 351-364, 2000.

[8] M. P. Ribeiro, D. J. Ewins, D. A. Robb, Non-Stationary Analysis and Noise Filtering Using a Technique Extended from the Original Prony Method, Mechanical Systems and Signal Processing, vol. 17, no. 3, pp 533-550, 2003.

[9] J. Ren, R.G. Vaughan, Model-Based Sonar Motion Compensation for Bottom Reverberation Coherence, IEEE Journal of Oceanic Engineering, vol. 35, no. 4, pp 887-894, 2010.

[10] D. W. Tufts, R. Kumaresan, Estimation of Frequencies of Multiple Sinusoids: Making Linear Prediction Perform Like Maximum Likelihood, Proc. of the IEEE, vol. 70, no. 9, pp 975-990, 1982.

[11] Hydrographic Dictionary, Part I,Volume I, Special Publication No. 32, 5th Edition, International Hydrographic Bureau, Monaco 1994.

[12] IHO Standards for Hydrographic Surveys 5th Edition, Special Publication No. 44, International Hydrographic Bureau, Monaco 2008.